ARMA 24–0591

Concept Feasibility and Predicted Behavior of Mining a Rock Tower with Drill-and-Blast Undermining Using Dynamic Three-Dimensional Discontinuum Numerical Models

Abousleiman, R.
Knight Piésold and Co., Denver, Colorado, USA
Contreras, C.I.
Stantec, Lima, Lima, Peru
Cremeens, J.
Knight Piésold and Co., Fort Collins, Colorado, USA
Worsey, T.
DynoConsult, New Castle, NSW, Australia
Rouse, N.
Thoroughbred Drill and Blast Consultants, Thurles, Tipperary, Ireland

ABSTRACT: The safety and efficacy of a proposed novel mining method - felling a mineralized rock tower away from an adjacent river and towards an existing open pit using a wedge-shaped "key-cut" blast pattern and post-split hinge – was analyzed by integrating site-specific and site-adjacent data to develop a into a dynamic three-dimensional discrete element method numerical model. These data included historic laboratory testing and geomechanical core logging from the adjacent open pit, Lidar scans and geomechanical spot mapping of the rock tower, local signature blast seismic data, and proposed blast-pattern. Static and dynamic model stages were run to assess the pre-blast, syn-blast, and post-blast deformation of the mineralized rock tower. Model sensitivities to mesh size, dynamic time-step, block size, and joint strength were assessed. Ultimately, model results indicated that the proposed mining method would likely result in 97 percent retention of the blasted material within the existing open-pit, and only 3 percent of material would be cast towards the adjacent river.

1. INTRODUCTION

The Dragon's Tooth rock tower is located near the base of an existing open pit at Mine A along the bank of a perennial river (Figure 1). The rock tower extends 50 meters (m) vertically above the open pit bottom and ranges in diameter from approximately 20 m at the crown to approximately 40 m at its basal contact with the adjacent open pit. The Dragon's Tooth and underlying material contain gold ore but were not mined with the completion of the open pit due to limited safe access for conventional open-pit mining equipment.

Successful mining of the Dragon's Tooth depends on limiting the casting and sliding of large blocks (i.e., blocks that require re-blasting) towards the river and the volume of fill required for access. This will afford more ore recovery and avoid blocking the river for a prolonged period. Mine A contacted Dyno Consult (DC) to develop a method to safely collapse the mineralized tower away from the river. DC developed a wedge-shaped "key-cut" blast pattern (Figure 2) and post-split hinge to topple the rock tower towards the open pit. The safety and efficacy of the proposed method was assessed using numerical models.

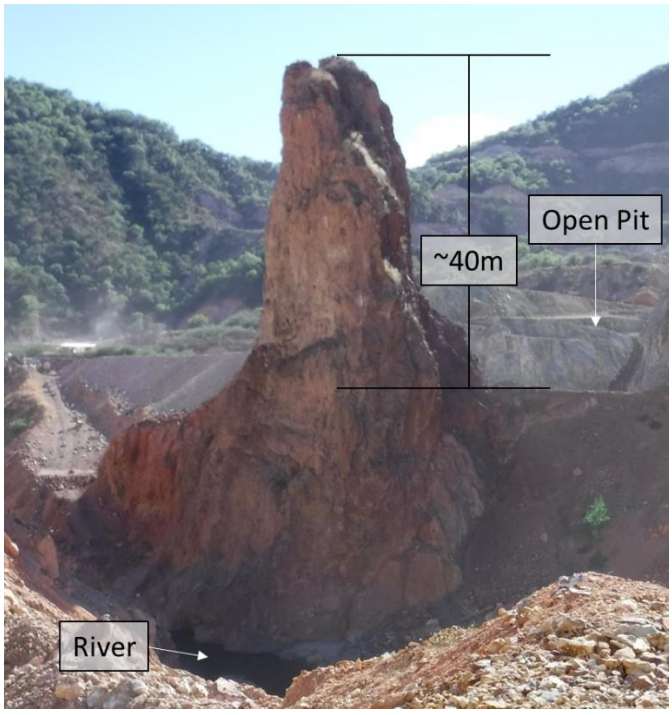

Fig. 1. Overview photograph of the Dragon's Tooth rock tower, perennial river, and open pit, facing south.

The models developed in support of this evaluation utilized point cloud and survey data provided by the mine, and photogrammetry and blast data provided by DC.

Rock mass characterization data from previous slope stability evaluations at the open pit (SRK Consulting [SRK], 2009; Knight Piésold, 2015) were coupled with site-specific observations collected during a site visit in November 2021 (Knight Piésold, 2022).

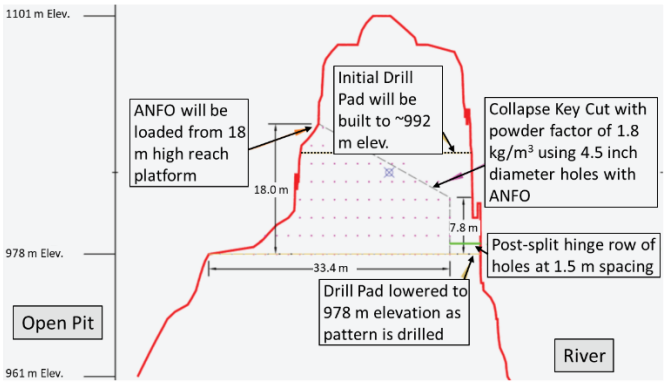

Fig. 2. Section view of the proposed "key cut" blast pattern and post-split hinge (modified from DC, 2022), facing northwest.

The available data was used to develop a three-dimensional discrete element method (DEM) numerical model using the three-dimensional distinct element code (3DEC) (Itasca Consulting Group, Inc. [Itasca], 2022). The modeling was conducted in two phases; first a static model was used to determine appropriate discontinuity rock bridging conditions. Then, dynamic models explicitly incorporated anticipated blast waveforms based on processed signature blast data from DC. Sensitivity analyses were also conducted to assess the impact of mesh size, smaller block sizes, zero discontinuity rock bridging, and orientation of peak particle velocity components on model results.

1.1. Geologic Site Setting

The Dragon's Tooth rock tower was formed by hydrothermal alteration of volcanoclastic sandstone and conglomerate as well as dacitic porphry and lithic crystal tuff. These lithologies have been hydrothermally altered by silicic-style alteration, which is also responsible for ore emplacement. Silicic alteration replaces softer minerals like plagioclase with silica. Ultimately, intact rock properties are more a function of alteration than parent lithology. Silicic alteration typically increases the strength and stiffness parent lithologies and can anneal previously low rock mass quality zones. The adjacent river runs along the strike of a northwest trending normal fault associated with mineralization and alteration.

2. AVAILABLE DATA

2.1. Laboratory Data

Knight Piésold previously conducted a pit slope stability evaluation for the adjacent open pit based on two rounds of geomechanical coreholes and laboratory testing (SRK, 2008; Knight Piésold, 2015). A total of 32 uniaxial compressive strength (UCS) tests were conducted to characterize intact rock strength of lithologies encountered in the open pit. Five UCS samples were also tested for elastic properties (i.e., Young's modulus (E) and Poisson's ratio). A total of eight, three-point (i.e., three different normal stresses) small-scale direct shear (SSDS) tests were conducted to estimate the shear strength properties of the rock discontinuities in the open pit. Normal stresses between 172 kilopascals (kPa) to 2,067 kPa were tested on both natural and saw-cut discontinuities.

While not directly taken from the Dragon's Tooth rock tower itself, many of the samples analyzed in support of adjacent pit development represent the same lithologies and alteration styles present in the rock tower. These laboratory test results (Table 1), coupled with engineering judgement, were used in defining the intact rock properties and discontinuity strengths implemented in the Dragon's Tooth rock tower numerical model.

Table 1. UCS and Elastic Properties Lab Testing Summary.

Sample ID	Density (kg/m3)	UCS (MPa)	Young's Modulus (GPa)	Poisson's Ratio
UCS-1	2,562.9	155.1	38.6	0.215
UCS-2	2,459.0	88.7	56.1	-
UCS-3	2,416.7	29.3	11.9	0.190
UCS-4	2,577.4	177.9	62.9	0.174
UCS-5	2,659.6	16.3	15.8	-

Table 2. SSDS Lab Testing Summary

Test	Friction Angle (°)	Cohesive Intercept (kPa)[1]
Natural Joint-1	34.7	89.7
Saw Cut-1	29.8	-1.4
Saw Cut-2	19.8	83.7
Saw Cut-3	28.1	-22.8
Saw Cut-4	28.2	32.8
Saw Cut-5	24.3	17.4
Natural Joint-2	39.3	4.3
Saw Cut-6	29.5	9.9

1. Cohesive intercept calculated by laboratory was assumed to be 0 during data reduction and friction angles were reinterpreted using a zero y-intercept best-fit.

2.2. Major Discontinuity Orientations

Mine A personnel collected four LiDAR scans using a Maptek LiDAR scanner with a combined total of approximately 65 million points. While the point density varied due to access, the major areas of interest, which included the southwest, southeast, and northeast sides of the tooth were well-represented in the point cloud data set. Mine A used Maptek PointStudio (Maptek 2020) to identify 11 major, through-going discontinuities. CloudCompare v2.11.3 (CloudCompare 2021) was used to confirm the orientation and location of the 11 major discontinuities. Select discontinuities are depicted in

Figure 3 and the orientation and geometries of all discontinuities are listed in Table 3.

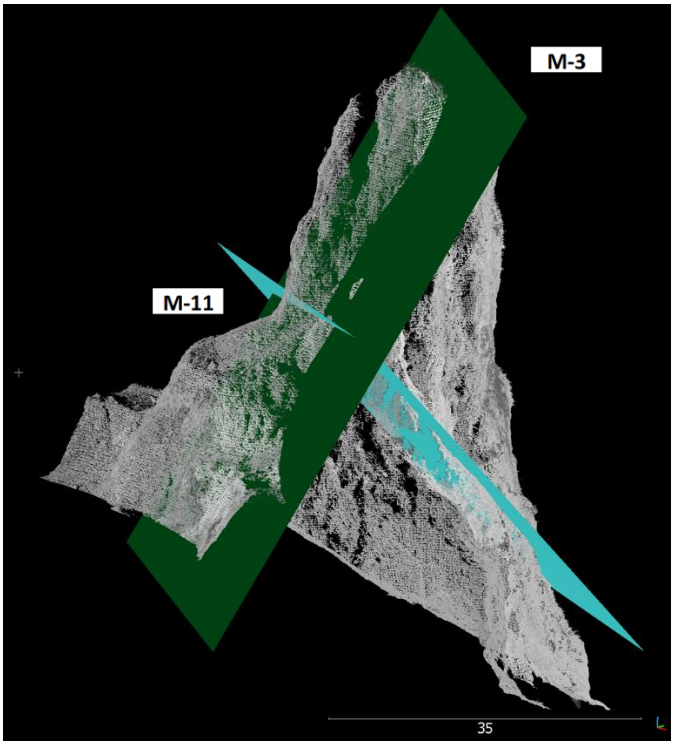

Fig. 3. Dragon's Tooth lidar scan and throughgoing discontinuity mean planes identified by Mine A personnel and confirmed by Knight Piésold, facing northwest.

Table 3. Major Discontinuity Orientations

Discontinuity ID	Plane Orientation	
	Dip (°)	Dip Direction (°)
M-1	50.2	223.2
M-2	89.4	6.3
M-3	62.0	222.0
M-4	77.2	40.6
M-5	83.3	356.5
M-6	87.5	343.1
M-7	55.5	235.3
M-8	87.5	69.7
M-9	45.7	118.9
M-10	79.7	114.8
M-11	46.5	32.6

2.3. Development Sequence and Blast Data

In otder to assess the stability of mining the tower, DC provided development details (e.g., CAD surfaces, cross-sections, drill pad elevations), and directed Mine A personnel to collect data seismic data from confined and unconfined signature blasts near the rock tower, and provided a blast design and analysis letter (DC 2022).

The development sequence includes a key cut (i.e., wedge) with an 18 m high face on the southwestern side of the tooth and 7.8 m high on the northeastern side of the tooth. The key cut will be blasted with 1.8 kilograms per cubic meter (kg/m^3) powder factor in 4.5 in diameter holes with 1.6 m of burden and a 2.5 m spacing. The proposed blast will propagate from southwest to northeast on a 10 millisecond (ms) delay between the 92 individual blastholes sequenced as shown in Figure 4.

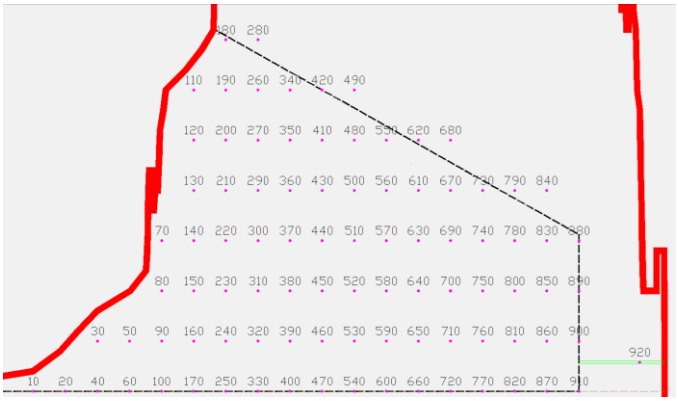

Fig. 4. Dragon's Tooth initiation sequence and timing.

The sequence also includes a post-split blast of the remaining portions of the tooth to create a "hinge" and promote the toppling of the tower towards the open pit. DC estimated the amount of blasted material that would clear the key cut (i.e., throw) using a simplified kinematic approach. This resulted in all blast holes 16 m from the southwestern face of the key cut will cast outside the key cut. This amounts to 62 percent of the key cut will be cast towards the southwest and 38 percent of the material at the northeast edge will remain in place. This cast geometry was slightly altered to account for any sloughing of blasted material, which could not maintain a vertical face.

Two signature shots were conducted by Mine A personnel at the direction of DC. A signature shot consists of a single blast that is representative of the proposed blast (i.e., similar geometry, charge, geology) that is monitored via seismographs at 20, 30, 40, and 50 m distances to record how the resulting waveform decays with time and distance from the blast. DC interpreted the results of confined and unconfined signature shots to determine their most conservative estimation of peak particle velocity (PPV) Eq. (1) and peak ground acceleration (PGA) Eq. (2) with respect to distance from the blast (x) as:

$$PPV\ (in/sec) = 26e^{-0.05x} \quad (1)$$

$$PGA\ (g) = 52e^{-0.08x} \quad (2)$$

Initial review of the expected PGA indicated that a pseudostatic analysis would be too conservative for the short blast duration and that a dynamic analysis applying the expected blast wave for the expected duration of the blast was more appropriate.

DC superimposed the most conservative signature shot to model the proposed blast using proprietary waveform superposition software. This resulted in the waveform that was used in the dynamic numerical model to explicitly simulate the potential effect of the proposed blast on the rock tower.

3. SITE VISIT

Knight Piésold personnel conducted a site visit to confirm that the available data accurately represented the conditions at the rock tower through geomechanical spot mapping. In particular, the joint conditions (i.e., aperture, infilling, and roughness) of the mapped discontinuities were documented and additional throughgoing discontinuities were identified.

During the geomechanical spot mapping field strength index was measured using the International Society for Rock Mechanics (ISRM) method (1987). More than one blow from a geologic hammer was required to fracture the intact rock throughout the tower. This corresponds with a field strength index of R4 and an approximate UCS of 50 to 100 megapascals (MPa), consistent with the historic laboratory data. Rock quality designation (RQD) (Deere 1988) and geologic strength index (GSI) (Marinos and Hoek 2002) were then determined to be approximately 80 percent and 65 to 76, respectively, exclusive of any isolated, major discontinuities.

Following observations of intact rock properties and overall rock mass properties, specific discontinuities previously identified by Mine A personnel and other previously unidentified features at the rock tower were inspected. The majority of the 11 discontinuities identified by Mine A and listed in Table 3 were observed from a distance due limited accessibility. However, a 5 cm thick clay filled joint was observed immediately below M-7. White staining was identified in M-7 in drone photographs suggesting that the clay gouge is partially continuous. M-3 did not appear to have significant infilling based on observations from the site inspection and drone photographs.

Discontinuity M-11 was observed to be dipping towards the river and daylighting on the northeastern side of the tower. The discontinuity surface was observed to be locally rough and globally undulating with moderate wall alteration and no significant infilling. These discontinuities were of significant interest because they have the potential to promote movement of larger portions of the tower towards the river as a result of blasting. All discontinuities were stable under current conditions, despite their steep dip. This suggested that the strength of the discontinuities is not purely frictional and some degree of rock bridging or large asperities are present.

4. NUMERICAL MODELING

In order to consider the three-dimensional nature of the Dragon's Tooth development, as well as the dynamic, discontinuity-driven deformation mechanisms the three-dimensional discrete element method (DEM) software 3DEC (Itasca 2022) was selected. 3DEC allows for consideration of explicit, fully separable fractures planes and can incorporate dynamic loading conditions such as blast waves into the model solution.

Given the low states of in situ stress and competent intact rock, the explicit strength of the intact portions of the Dragon's Tooth rock tower were excluded from the numerical modeling stability analysis and the linear-elastic constitutive model was used to represent intact rock. Deformation impacting safety and efficacy of the proposed development will be dominated by the discontinuities present and their behavior during changing loading conditions due to blasting.

Based on the measured dip, joint condition observations, and overall stable condition of the rock tower, some degree of rock-bridging (i.e., non-continuous joints) must be present in all the currently daylit discontinuities. The magnitude of rock bridging (i.e., cohesive and tensile strength, or large amplitude undulations) should be conservatively accounted for through back-analysis because determination of rock bridging in-situ is not possible. Friction angles determined from SSDS testing of natural and saw cut joints were selected for modeled peak and residual friction angles. Multiple joints identified by Mine A personnel have very similar orientations and locations within the rock tower. The most critical (i.e., steepest dip or largest block) of these redundant joints were selected to include in the modeling.

4.1. Model Geometry

Two main geometries were considered through the course of the numerical modeling in support of the stability evaluation, the existing geometry, and the key cut blast geometry. Both were developed based on the existing site survey contour lines and the proposed development provided by DC and Mine A.

The existing geometry site survey contours were extremely detailed and required some simplification to successfully construct the 3DEC model geometry. This involved manual removal of contour polyline nodes (Figure 6).

The final adjustment to the given geometry was the boundary between the material in the proposed key cut blast that will fully cast and the material that will remain as calculated by DC (2022). It was assumed that the blasted material, while unable to cast, would slough at a reasonable angle of repose in the key cut (Figure 7).

Following the construction of the model geometry, the mapped discontinuities listed in Table 3 were included in

the model geometry as explicit, fully continuous planes. Additional horizontal slice discontinuities were included approximately every 10 m to facilitate model construction

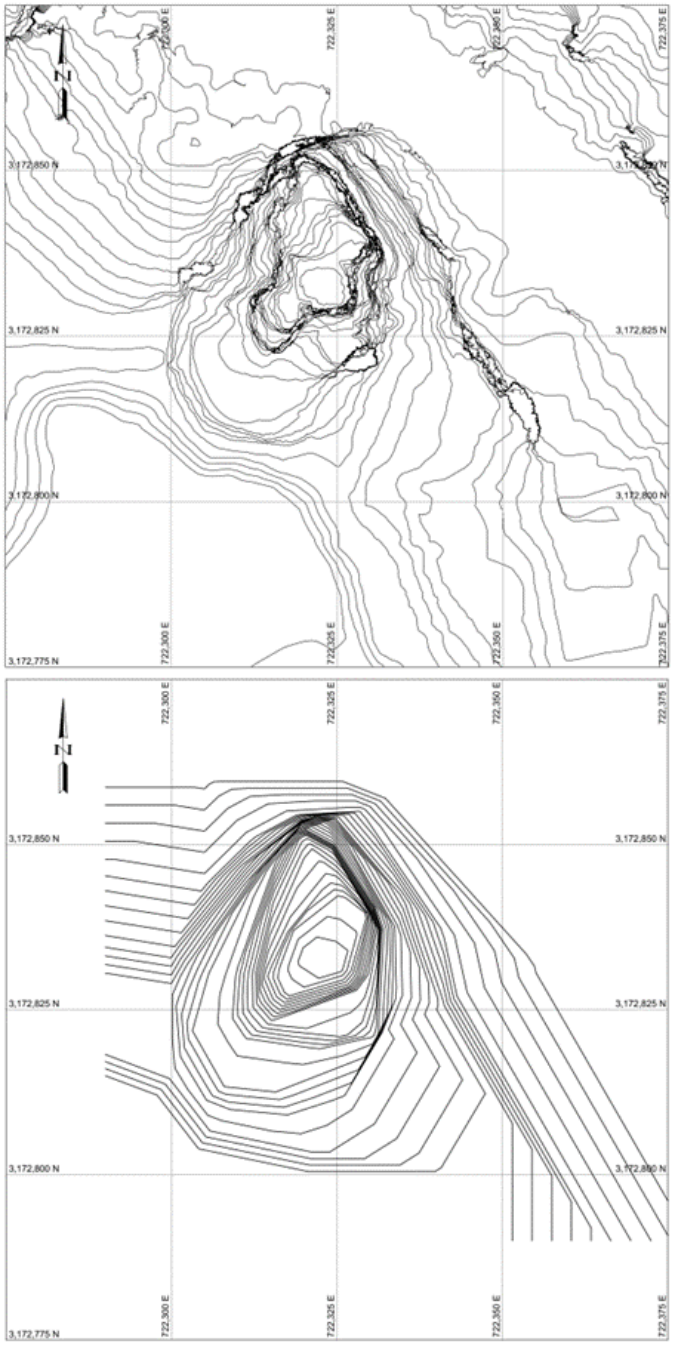

Fig. 6. Original (top) and simplified (bottom) contours for 3Dec model geometry development.

and meshing. In dynamic models, additional joints were added parallel to three of the discontinuities (i.e., M-3, M-6, and M-11) listed in Table 3 to assess the effect of increased blockiness on the efficacy of the development. These additional joints were modeled with an average spacing of 5 m.

All models featured a graded mesh with a maximum zone size of 3 to 4 m at the periphery (i.e., drilling platform, model base, tooth below 978 masl) and 2 m towards the areas of interest (i.e., key cut boundary and above).

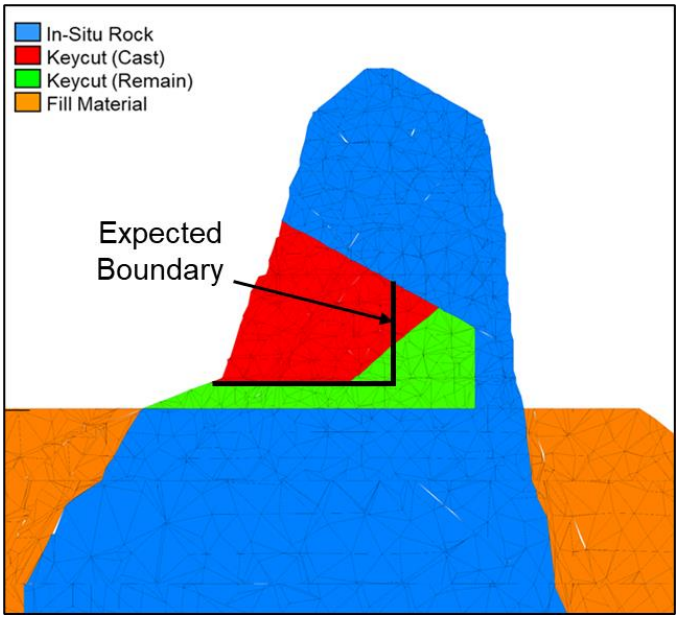

Fig. 7. Model geometry showing expected cast-remain boundary in keycut, with the adjusted model.

4.2. Constitutive Models

3DEC model inputs were based on interpretation and integration of historic laboratory testing, site investigation observations, and numerical modeling back-analyses as described in the following sections. Intact block materials were represented using the Isotropic Linear-Elastic constitutive model and discontinuities were modeled using the Mohr-Coulomb Residual Strength constitutive model. Discontinuity strength was predominantly frictional, with the appropriate amount of cohesion and tensile strength applied to portions of discontinuities as determined through back-analysis described in Section 5.

4.3. Intact Material Properties

Due to the extremely strong nature of the silicic alteration, and the low levels of confining stress, the deformation of the tower will be dominated by the existing discontinuities present throughout. Furthermore, the lithologies present feature no significant fabric or anisotropy. This allows for the intact portions of the tower to be accurately represented using an isotropic, linear-elastic constitutive model. Average Young's Modulus (34.0 GPa), Poisson's ratio (0.2) and density (2,600 kg/m^3) values obtained from five UCS tests conducted by SRK (2009) were applied to the intact rock blocks in the numerical model. The fill material used in constructing the drill pad was assigned the same material properties as intact rock to increase computational efficiency of the numerical model. Due to the large size of the drill pad, using an inelastic constitutive model or softer elastic material properties would increase model run-time significantly. Given that the tower is stable under current conditions and that no discontinuities daylight within 5 meters of the top of the drill pad, deformation of the drill pad is unlikely and will not significantly impact the safety or efficacy of the proposed development.

The stiffness of the material that may remain in the key cut following the blast should be more accurately represented as it is likely to affect the deformation of the tower following the key cut blast. Since the remaining material is likely to be fully yielded due to the blasting, the deformation of the remaining material can be represented with a softer elastic material. Parameters for fill material were selected based on experience with similar geomaterials resulting in a Young's Modulus of 0.5 GPa, density of 2,100 kg/m^3, and Poisson's Ratio of 0.2.

4.4. Discontinuity Material Properties

All discontinuities in the numerical model consist of contacts that are fully continuous and smooth (i.e., no large-scale roughness) planes. Every contact is further divided into sub-contacts which can each have their own explicit joint properties. The peak and residual frictional strength, joint shear stiffness, and joint normal stiffness of the subcontacts in the tower were based on the natural (i.e., peak) and saw cut (i.e., residual) SSDS lab testing contracted by Knight Piésold (2015) and SRK (2009). The input parameters selected and calculated from the laboratory test results were a peak friction angle of 39.0 degrees, residual friction angle of 30.0 degrees, normal stiffness of 25.0 GPa/m, and shear stiffness of 2.5 GPa/m. Peak cohesion, residual cohesion, tensile strength, and dilation angle were all set to 0.

Non-mapped discontinuities used to facilitate construction of the model and the duplicate joints of M-3, M-6, and M-11 were assigned subcontact properties that included cohesion and tensile strengths of 0.5 MPa and 0.1 MPa, respectively. This effectively modeled for a value of 10 percent rock bridging with a more consistent and repeatable method.

4.5. Stress Initialization and Static Back-Analyses

Multiple model stages, methods, and boundary conditions were used to evaluate the existing stability of the tower and the efficacy of the proposed blast.

The first model stage in both the existing conditions and proposed key cut blast models applied fixed zero-velocity boundary conditions normal to the respective x, y, and z faces at the base of the model. Then gravitational acceleration was applied, and stresses were initialized using the topography of the model, material density, and a horizontal stress ratio of 1.0. The model was then solved to a standard equilibrium solution ratio of $(10)^{-6}$. Review of the equilibrium displacements, velocities, and stresses confirmed that model stress initialization was realistic, and that further modeling could be conducted.

4.6. Discontinuity Strength Back-Analysis

Given that the tower is stable in its current condition, and most of the mapped discontinuities are dipping greater than the selected peak friction angle of 39.0 degrees, it follows that some appreciable amount of rock bridging is present along the discontinuities in the tower. Rock bridging can either be in the form of an impersistent, but smooth joint, or large-scale roughness (i.e., undulation) of a fully persistent joint. Regardless of the mechanism the result is largely the same where a given joint will require additional shear stress to yield and fail by breaking through or riding over rock bridging.

To evaluate the amount of rock bridging present in the rock tower discontinuities, conservative values of cohesion (5 MPa) and tensile strength (1 MPa) were applied to randomly selected sub-contacts in the existing geometry model. These values were established based on laboratory strength testing of intact rock (Knight Piésold 2015, SRK 2009) and engineering judgment. The cohesion is approximately 10% of the UCS, whereas the tensile strength equals 20% of the cohesion. To stabilize the tower under existing conditions, 10 percent of the subcontacts of each contact required rock bridge strength properties. Note that in the key cut blast analysis models no mapped discontinuities represented in the model were assigned rock bridge strength and they were modeled as purely frictional joints. The presence of the drilling platform in the key cut blast geometry prevented the daylighting of nearly all the mapped joints, which prevented the frictional strength from being exceeded during static stages of the model. This allowed for the most conservative representation of mapped joint strength up to, during, and after the blast.

Following establishment of the minimum rock bridging to maintain stability under existing conditions, the assessment of the key cut blast efficacy was conducted.

4.7. Dynamic Model

Following stress initialization and static model equilibrium, the dynamic mode in 3DEC was enabled and the fixed zero-velocity boundary conditions applied normal to the respective faces of the model base were changed to viscous boundary conditions. These changes to the model methodology and boundary conditions allowed explicit consideration of the blast wave as provided by DC and allow for realistic energy dissipation away from the areas of interest at the model boundaries.

The proposed key cut cast material, as shown in Figure 7 was deleted from the model and the longitudinal, transverse, and vertical PPV were applied to the internal boundary of the key cut between the uncast material and the remainder of the rock tower as an applied velocity vector. A 26 times multiplier was applied to the superimposed waveform using the equation provided by DC. This resulted in an overestimation of the blast wave by assuming that no reduction in blast wave PPV occurred between the blasthole and the key cut boundary.

The model was then run for one second, approximately 50 milliseconds longer than the superimposed blast waveform. As the model stepped forward the applied velocities would change with the waveforms. During this stage, the x, y, and z velocity at the top of the key cut boundary and the top of the rock tower were recorded to verify that the blast wave had been applied properly and that the velocities were attenuating realistically. The applied velocity vectors at 0.25 seconds of dynamic model runtime, as well as the applied waveform are shown in Figure 8.

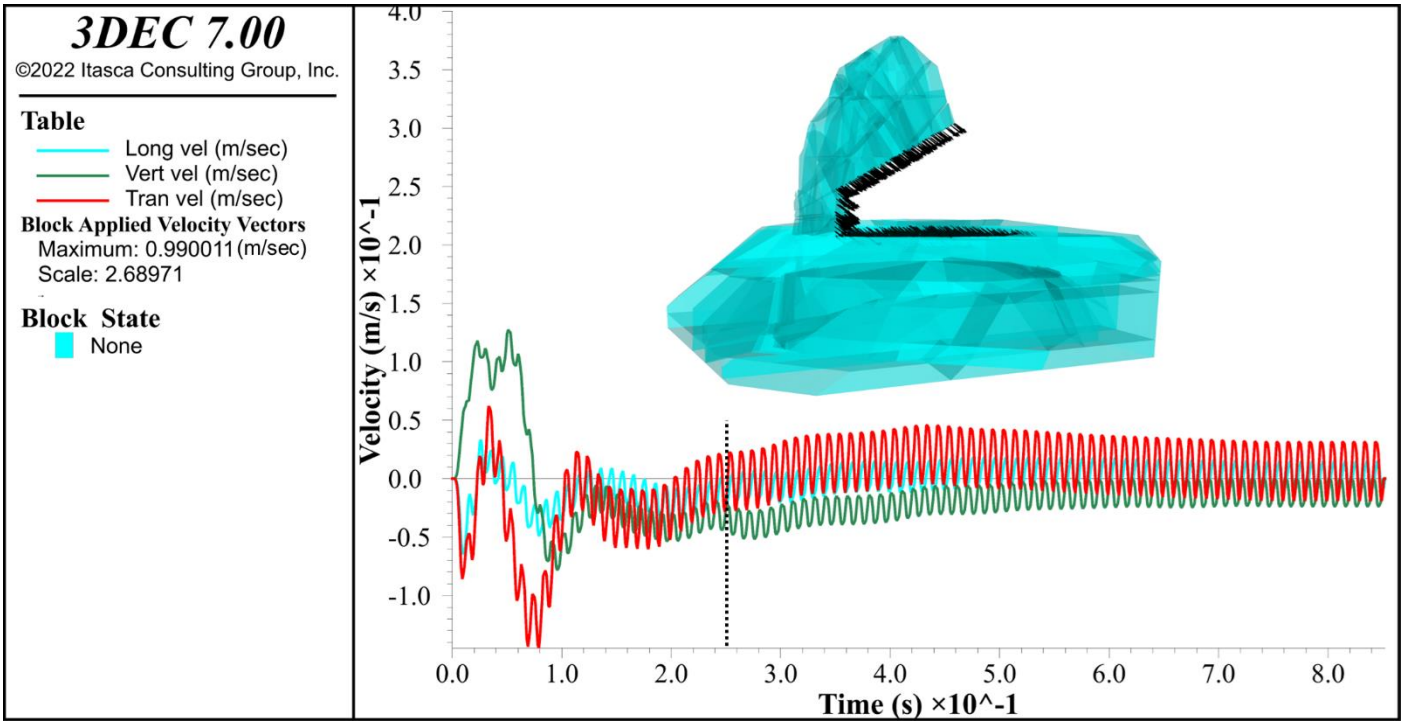

Fig. 8. Key-Cut Blast Applied Waveform Graph and Applied Velocity Vectors at 0.25 Seconds of Dynamic Simulation Time.

After the one second of dynamic model runtime was complete, the dynamic mode was turned off, the applied velocity at the key cut boundary was removed, and the model boundary conditions were restored to their zero velocity state from the pre-dynamic stress initialization stage. The model was then solved to a standard equilibrium solution ratio and the volume of blocks that fell towards the open pit and towards the river were recorded.

5. DISCUSSION

The results of the dynamic analysis indicate that vibrations generated by blasting would not produce significant deformations that could lead to the rock tower collapsing towards the river. Instead, during this stage, only a few rock blocks would move towards the river with a maximum displacement of 4.5 m in the north direction, and most of the rock tower would not show significant movement (i.e., displacements are less than 1 m) in any direction by the end of the dynamic simulation (i.e., 1.0 seconds). Figure 9 shows displacement vectors and displacement contours at 0.25 seconds of the dynamic simulation. The applied waveform was based on the compounded waveform and distance decay formula provided by DC. This conservatively assumed that the blast occurred at every part of the key cut boundary simultaneously. In reality, only the blastholes near the key cut edge would impart such a load, and the waves generated from blastholes near the center of the key cut would decay as they approached the key cut boundary.

Figure 10 shows the collapse of the rock tower following post-dynamic static analysis. Once the key cut is blasted and cast, the rock tower collapses because of the effect of gravity in the manner intended and according to DC's design. According to the post-dynamic static analysis results, the upper portion of the rock tower would topple in direction of the open pit and fall on the 978 m amsl drill platform. The un-cast portion of the key cut would have a negligible effect on the trajectory of the falling blocks of rock. The northern portion of the Dragon's Tooth rock tower would displace to the north (towards the river) with most rock blocks remaining on the drill platform and a few others falling into the river. By the end of the simulations (Figure 10), up to 2.9 percent of the rock blocks fell into the river and 97.1 percent remained on the drill platform.

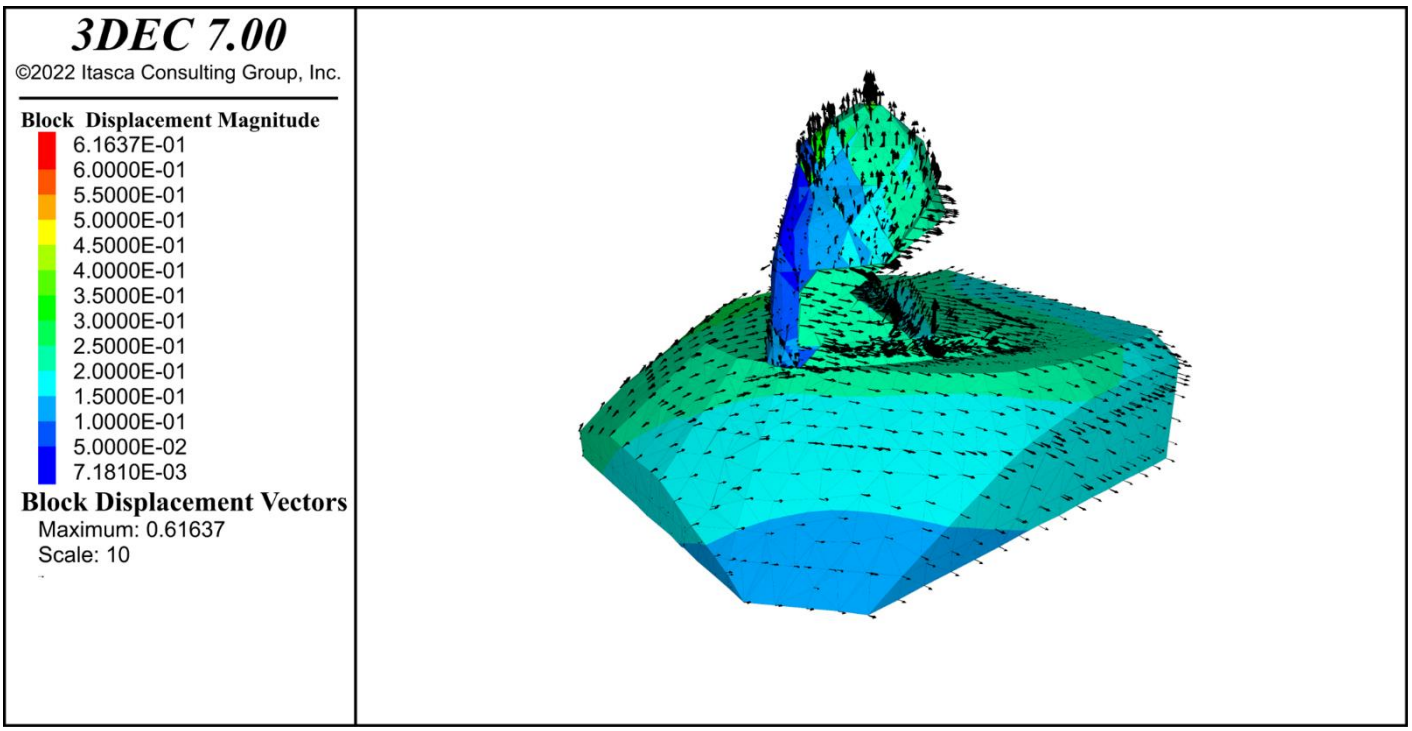

Fig. 9. Key-Cut Blast Dynamic Analysis, Displacement Vectors (m) and Contours (m) at 0.25 Seconds of Dynamic Simulation Time

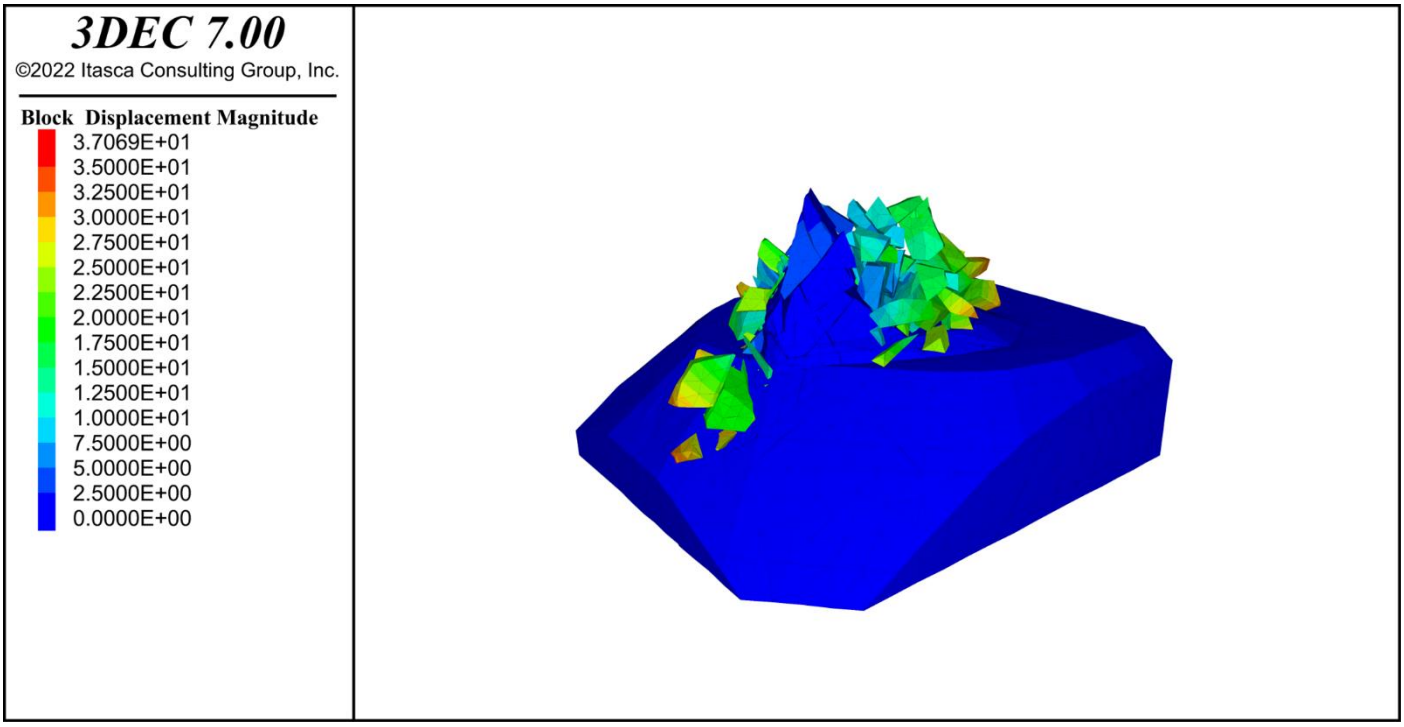

Fig. 10. Key-Cut Blast Post-Dynamic Static Analysis, Rock Tower Collapse Sequence (96.5 Million Steps) Final Equilibrium Displacement Contours (m).

6. CONCLUSIONS AND FUTURE WORK

Conceptual evaluation of the safety and efficacy (i.e., post-blast spatial configuration of rock blocks) of proposed felling of the Dragon's Tooth rock tower was conducted. A proof-of-concept numerical model was undertaken to approximate the possible post-blast spatial configuration of the fallen rock blocks of the blasted tower. The three-dimensional DEM implemented in 3DEC (Itasca 2022) was used to create the appropriate geometry and mesh, then representative material properties and boundary conditions were assigned. Using both static and dynamic solution modes, Knight Piésold evaluated multiple model stages including stress initialization, existing conditions joint strength back-analysis, dynamic explicit blast waveform, post-dynamic static collapse, and model sensitivities to the orientations of the applied waveform.

The final model results indicated that the post-blast spatial configuration of rock blocks was greater than 97 percent from above the 978 m amsl level landing on the drill platform or towards the open pit.

It is assumed that blast gas pressures will not impose significant reduction in normal load within the tower and that gas pressures will largely dissipate towards unconfined faces of the Dragon's Tooth. The analysis also assumed that controlled blasting techniques will be practiced to maximize fragmentation and casting and minimize gas pressure and PPV.

Future stages of design will refine the application of the blast wave and assess the impact of inelastic fill, various cast-remain post-blast geometries, and other joint constitutive models such as continuously yielding or Barton-Bandis.

REFERENCES

1. CloudCompare v2. (2022). v2.12.4.
2. Deere, D. (1988). The rock quality designation (RQD) index in practice. In *Rock classification systems for engineering purposes.* ASTM International.
3. DynoConsult. (2022). *[Dragon's Tooth rock tower] Blast Design and Analysis.* Letter Report. Draft 3.
4. ISRM. (1987). A presentation of the ISRM Suggested Methods for determining fracture toughness of rock material. In *6th ISRM Congress*.
5. Itasca Consulting Group. (2022). 3DEC Version 7.00.150. 3DEC 7.0 Documentation.
6. Knight Piésold and Co. (2015). [Mine A Open Pit] Design Report. Rev 0.
7. Maptek. (2020). PointStudio.
8. Marinos, P. and Hoek, E. (2002). GSI: A Geologically Friendly Tool for Rock Mass Strength Estimation.
9. SRK Consulting. (2009). [Mine A Open Pit] Report